Applied & Computational Mathematics

Mohamad et al., J Appl Computat Math 2015, 4:6
DOI: 10.4172/2168-9679.1000261

Research Article Open Access

# Local Non-similarity Solution for MHD Mixed Convection Flow of a Nanofluid Past a Permeable Vertical Plate in the Presence of Thermal Radiation Effects

**Mohamad R[1], Kandasamy R[1]* and Ismoen M[2]**

[1]*Faculty of Science, Technology and Human Development, University Tun Hussein Onn Malaysia 86400 Parit Raja, Batu Pahat, Johor, Malaysia*
[2]*Engineering Mathematics Unit, Faculty of Engineering, Brunei Institute of Technology, JalanTungku Link Gadong BE1410, Negara Brunei Darussalam*

## Abstract

Combined heat and mass transfer on mixed convection non-similar flow of electrically conducting nanofluid along a permeable vertical plate in the presence of thermal radiation is investigated. The governing partial differential equations of the problem are transformed into a system of non linear ordinary differential equations by applying the Sparrow–Quack–Boerner local non-similarity method (LNM). Furthermore, the obtained equations are solved numerically by employing the Fourth or fifth order Runge Kutta Fehlberg method with conjunction to shooting technique. The profiles of flow and heat transfer are verified by using five types of nanofluids of which metallic or nonmetallic nanoparticles, namely Copper (Cu), Alumina ($Al_2O_3$), Copper oxide (CuO), silver (Ag) and Titanium ($TiO_2$) with a water-based fluid. Rosseland approximation model on black body is used to represent the radiative heat transfer. Effects of thermal radiation, buoyancy force parameters and volume fraction of nanofluid on the velocity and temperature profiles in the presence of suction/injection are depicted graphically. Comparisons with previously published works are performed, and excellent agreement between the results is obtained. The conclusion is that the flow fields is affected by these parameters.

**Keywords:** Nanofluids; Local nonsimilarity method; Mixed convection; Magnetic field; Thermal radiation

## Introduction

The thermal conductivity of heating or cooling fluids is a very important property in the development of energy-efficient heat transfer systems. In all processes involving heat transfer, the thermal conductivity of the fluids is one of the basic properties taken account in designing and controlling the process [1]. However, the traditional pure liquid heat transfer medium has a low thermal conductivity, which limits the heat transfer enhancement. Therefore, it is necessary to prepare a higher thermal conductivity and more efficient heat transfer medium. Scientific breakthrough has been made by Choi in 1995 when for the first time he introduced the term "Nanofluids". Nanofluids are a new class of heat transfer fluids with substantially higher conductivities. These fluids are developed by suspending nanoscale metallic or nonmetallic particles in the base fluid [2]. In recent years, studies on nanofluids has been receiving a lot of attention worldwide due to its unique properties which make them potentially useful in many applications in heat transfer, including microelectronics, fuel cells, pharmaceutical processes, and hybrid-powered engines [3]. Many studies on nanofluids are being conducted by talented researchers such as Abu-Nada [4-11].

Magnetohydrodynamic (MHD) is the study of electrically conducting fluids as they move in a magnetic field. As the magnetic field cutting the moving fluid changes, an electric current is induced in the fluid [12]. The study of MHD flow and heat transfer are deemed as of great interest due to the effect of magnetic field on the boundary layer flow control and on the performance of many systems using electrically conducting fluids. Some of the engineering applications are in MHD power generators, plasma studies, cooling of nuclear reactor, gas turbines, geothermal energy extractions, purifications of metal from non-metal enclosures, polymer technology, the boundary layer control in aerodynamics, crystal growth and metallurgy [13]. Magnetic nanofluid is a unique material that has both the liquid and magnetic properties. Many of the physical properties of these fluids can be tuned by varying magnetic field [3]. As the magnetic nanofluids are easy to manipulate with an external magnetic field, they have been used for a variety of studies. Magneto-hydrodynamic flow and heat transfer of electrically conducting and heat generating fluids through and over different types of modes, geometries and boundary conditions are research subjects that have interested and attracted many investigators in recent years. In free convection, Hamad et al. [14] discussed the problems of magnetic field effects on free convection flow of a nanofluid past a semi-infinite vertical flat plate. Study on boundary layer flow of a nanofluid over a permeable vertical plate in the presence of magnetic field, heat generation or absorption, suction or injection, Brownian motion of particles and thermophoresis effects have been studied by Chamka and Aly [15]. Mohammed [16] has investigated MHD free convection of a nanofluid over a vertical flat plate taking into account Newtonian heating boundary condition. While in forced convection, Wubshet Ibrahim and Shanker [17] have analyzed the boundary layer flow and heat transfer over a permeable stretching sheet due to a nanofluid with the effects of magnetic field, slip boundary condition and thermal radiation. By extending the work of Makinde and Aziz [18] has been investigated numerically the MHD laminar boundary layer slip flow of an electrically conducting nanofluid over a convectively

***Corresponding author:** Kandasamy R, Faculty of Science, Technology and Human Development, University Tun Hussein Onn Malaysia, 86400 Parit Raja, Batu Pahat, Johor, Malaysia, Tel: 6074537000; E-mail: future990@gmail.com

**Received** June 19, 2015; **Accepted** October 21, 2015; **Published** October 26, 2015

**Citation:** Mohamad R, Kandasamy R, Ismoen M (2015) Local Non-similarity Solution for MHD Mixed Convection Flow of a Nanofluid Past a Permeable Vertical Plate in the Presence of Thermal Radiation Effects. J Appl Computat Math 4: 261. doi:10.4172/2168-9679.1000261

heated permeable moving linearly stretching sheet taking in account the effects of Brownian motion, thermophoresis, magnetic field, and heat generation/absorption. Abdel-Gaied and Hamad [19] analyzed steady MHD forced convection flow of alumina-water nanofluid on moving permeable vertical flat plate with convective surface boundary condition. Meisam Habibi Matin and Pouyan Jahangiri [20] studied the effects of suction-injection and viscous dissipation on forced convection boundary layer MHD flow of a nanofluid over a permeable stretching. On the effect of MHD flow of nanofluids, although there are many studies regarding the natural and forced convections regime, there are only a few regarding the mixed convection regime. Chamkha et al. [15] studied the flow of mixed convection MHD flow of a nanofluid past a vertical stretching permeable surface in the presence of magnetic field, heat generation or absorption, thermophoresis, Brownian motion and suction or injection effects. Recently, the study on the effect of heat source/sink on steady MHD mixed convection boundary layer flow over a vertical permeable surface embedded in a porous medium saturated by a nanofluid was presented by Mohammad Mehdi Keshtkar et al. [21].

At high operating temperature, thermal radiation effect becomes significantly very important and cannot be ignored. Many engineering processes occur at high temperatures and hence the knowledge of thermal radiation plays a major role in designing pertinent equipment. As has been pointed out by previous scholars, magnetic nanofluid has many applications such as in magnetofluidic leakage-free rotating seals, magnetogravimetric separations, acceleration/inclinations sensors, aerodynamic sensors (differential pressure, volumetric flow), nano/micro-structured magneto rheological fluids for semi active vibration dampers, biomedical applications in plant genetics and veterinary medicine [16]. In view of these, several researchers have made contributions to the study of MHD flow of nanofluid with thermal radiation effect. Khan et al. [22] presented a similarity analysis for steady boundary layer flow of a nanofluid past a stretching sheet with the influence of magnetic field and thermal radiation. Poornima and Bhaskar Reddy [23] studied the simultaneous effects of thermal radiation and magnetic on heat and mass transfer flow of nanofluids over a non-linear stretching sheet. The study focuses on the numerical solution of a steady free convective boundary-layer flow of a radiating nanofluid along a non-linear stretching sheet in the presence of transverse magnetic field. Aini Mat [24] theoretically studied the steady magneto-hydrodynamic (MHD) mixed convection boundary layer flow of a stretching vertical heated sheet in a power law nanofluid with thermal radiation effect. Stanford Shateyi, et al. [25] have carried out the analysis of MHD boundary layer flow of a nanofluid over a moving surface in the presence of thermal radiation. Reddy [26] examined the influence of MHD and heat radiation on boundary layer flow of nanofluid over a stretching surface with velocity slip and convective boundary conditions. Very recently, Eshetu Haile and Shankar [27] investigated simultaneously the effects of magnetic field, thermal radiation, viscous dissipation, Ohmic effects and permeability of surfaces on heat transfer of nanofluid over a moving flat plate.

Many problems in boundary-layer flow and heat transfer are nonsimilarity. Nonsimilarity of boundary layers may stem from a variety of causes such as variation in wall temperature, variation in free-stream velocity, surface mass transfer, effect of suction or injection of fluid at the wall, the buoyancy force effect, inclination angle effects, etc., [28]. The nonsimilarity of boundary layer can also arise from by more than one factor. There are various numerical methods have been proposed to deal with such nonsimilar boundary layer problems and among them, the most well-known method is the local nonsimilarity method which was initiated by Sparrow et al. [28]. Since then it has been applied by several investigators to solve various non similar boundary layer problems. Muhaimin and Kandasamy [29] presented a study addresses the chemical reaction and magnetic effects on a nonlinear boundary-layer flow over a porous wedge in the presence of the buoyancy force and non-uniform pressure gradient. Akgu and Pakdemirli [30] investigated the effect of different types of nanoparticles on the heat transfer from a continuously moving stretching surface with power-law velocity and temperature.

However, to the best of authors' knowledge, no attempt has been made to solve the problem of non-similar MHD mixed convective heat transfer flow of nanofluids over a permeable vertical plate in the presence of thermal radiation effect using the local nonsimilarity method (LNM). Hence, the current research presents a local nonsimilarity method to obtain the general solution of a nonsimilarity partial differential equation of the problem with Runge-Kutta-Gill with shooting methods. This study extended the work by Watanabe [31] to the case of nanofluids taking into consideration of magnetic and thermal radiation effects. It is, thus, expected that the local nonsimilarity approach should yield more accurate results for the velocity and temperature fields than those of the local similarity model.

## Mathematical Analysis

A two-dimensional steady magnetohydrodynamic mixed convective boundary-layer flow of a viscous incompressible nanofluid over an isothermal vertical plate is considered in Figure 1. The fluid is assumed to be Newtonian, electrically conducting, constant fluid properties and moves on the top of the surface with a constant velocity $U_0$. We also assumed that there are thermal equilibrium between the base fluid (i.e., water) and the nanoparticles and no slip occurs. A uniform magnetic field of strength $B_0$ is applied normal to the plate. In this current work, the magnetic Reynolds number is assumed small, as is the case in most practical applications, and therefore the induced magnetic field is considered insignificant. Applying the nanofluid model proposed by Tiwari and Das [32] and employing the Boussinesq approximation, the governing equations describing the problem may be written as

$$\frac{\partial u}{\partial x}+\frac{\partial v}{\partial y}=0 \tag{1}$$

$$u\frac{\partial u}{\partial x}+v\frac{\partial u}{\partial y}=\frac{1}{\rho_{nf}}\left[\mu_{nf}\frac{\partial^2 u}{\partial y^2}\right]+\frac{(\rho\beta)_{nf}}{\rho_{nf}}g\left(T-T_\infty\right)-\frac{\sigma B_0^2}{\rho_{nf}}\left(u-U\right) \tag{2}$$

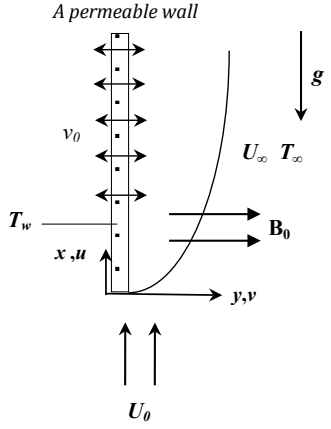


**Figure 1:** Physical model and flow analysis.

$$u\frac{\partial T}{\partial x}+v\frac{\partial T}{\partial y}=\alpha_{nf}\frac{\partial^2 T}{\partial y^2}-\frac{1}{(\rho C_p)_{nf}}\frac{\partial q_r}{\partial y} \quad (3)$$

subject to the boundary conditions:

$$u=0,\ v=-v_0\ (\text{constant}),\ T=T_w \text{ at } y=0: \quad (4)$$

$$u=U_\infty,\ T=T_\infty \text{ at } y\to\infty \quad (5)$$

A constant suction is imposed at the plate surface, as shown in Figure 1.

In Equs. (1) – (5), u and v are the corresponding velocity components in the x and y directions, $v_0$ is the suction velocity (constant). $U_\infty$ and $T_\infty$ are the velocity and temperature of free stream at outer edge of boundary layer and $\alpha_{nf}$ is a thermal diffusivity of nanofluid which are defined as

$$\alpha_{nf}=\frac{k_{nf}}{(\rho C_p)_{nf}} \quad (6)$$

The dynamic viscosity of the nanofluid, $\mu_{nf}$ and the density of the nanofluid, $\rho_{nf}$ are given by Brinkman [33] as

$$\rho_{nf}=(1-\phi)\rho_f+\phi\rho_s,\ \mu_{nf}=\frac{\mu_f}{(1-\phi)^{2.5}} \quad (7)$$

with ϕ is the nano-particle volume fraction of the nanofluid, $\rho_f$ is the density of the base fluid, $\rho_p$ is the density of the solid particle and $\mu_f$ is the viscosity of the base fluid [34]. Following the Maxwell-Garnetts model, the effective thermal conductivity of the nanofluid is given as [35].

$$\frac{k_{nf}}{k_f}=\frac{(k_s+2k_f)-2\phi(k_f-k_s)}{(k_s+2k_f)-\phi(k_f-k_s)} \quad (8)$$

and the heat capacitance of the nanofluid (ρCp) is defined as

$$(\rho C_p)=(1-\phi)(\rho C_p)_f+\phi(\rho C_p)_s \quad (9)$$

The subscripts f, s and nf in Equs. (6) – (9) denote properties of base fluid, nano-particles and nanofluid respectively. Under the concept of boundary layer theory, the thickness of boundary layer, δ(x) is defined as

$$\delta(x)=\sqrt{\frac{vx}{U}} \quad (10)$$

with dimensionless variable $\frac{u}{U_\infty}=f'(\eta)$

Following Watanabe [31] , we took the set of dimensionless transformations as

$$\psi(x,\eta)=(v_f x U_0)^{1/2} f(x,\eta),\eta=y\left(\frac{U_0}{v_f x}\right)^{1/2},\theta(x,n)=\frac{(T-T_\infty)}{(T_w-T_\infty)} \quad (11)$$

The continuity equations, Eq (1) is identically satisfied by defining a stream function ψ (x, y) such that

$$u=\frac{\partial\psi}{\partial y}\ and\ v=\frac{\partial\psi}{\partial x}$$

The velocity components can be expressed as

$$u=U_0\frac{\partial_f}{\partial_\eta},v=\left[f\frac{dq}{dx}+q\left(\frac{\partial f}{\partial x}+\frac{\partial f}{\partial\eta}.\frac{\eta}{p}.\frac{dp}{dx}\right)\right]$$

with q and p are defined as

$$q(x)=(v_f x U_0)^{1/2},p(x)=\left(\frac{U_0}{v_f x}\right)^{1/2}.$$

The radiative heat flux, $q_r$ is described by Rosseland approximation such as

$$qr=-\frac{4\sigma_1}{3k_1}\frac{\partial T^4}{\partial y} \quad (12)$$

where $\sigma_1$ and $k_1$ are the Stefan Boltzmann constant and the mean absorption coefficient, respectively. Assuming that the temperature differences within the flow are sufficiently small, the term $T^4$ can be expressed in a simpler way by using a Taylor's series as following approximation

$$T^n\approx(1-n)T_\infty^n+nT_n^{n-1}T \quad (13)$$

Using eq. (13), we have [36]

$$\frac{\partial q_r}{\partial y}=-\frac{4\sigma_1}{3k_1}\frac{\partial^2 T^4}{\partial y^2}\approx\frac{16T_\infty^3\sigma_1}{3k_1}\frac{\partial^2 T}{\partial y^2} \quad (14)$$

In order to transform Equs. (2) and ( 3) into ordinary differential equations, we substitute variables Equs. (6)-(9) and (11)-(14) into the system thus obtaining the following system of equations

$$\frac{1}{(1-\phi)^{2.5}\left[1-\phi+\phi\left(\frac{\rho_s}{\rho_f}\right)\right]}f'''+\frac{1}{2}ff''+\xi\theta-M(f'-1)=\xi\left[\frac{\partial f}{\partial\eta}\frac{\partial^2 f}{\partial\xi\partial\eta}-\frac{\partial f}{\partial\xi}\frac{\partial^2 f}{\partial\eta^2}\right] \quad (15)$$

$$\frac{1}{pr}\frac{\left(\frac{k_{nf}}{k_f}\right)}{\left[1-\phi+\phi\frac{(\rho C_p)_s}{(\rho C_p)_f}\right]}\theta''+\frac{1}{2(N+1)}\theta' f=\frac{1}{(N+1)}\xi\left[\frac{\partial f}{\partial\eta}\frac{\partial\theta}{\partial\xi}-\frac{\partial\theta}{\partial\eta}\frac{\partial f}{\partial\xi}\right] \quad (16)$$

where it has been recognized from the literature [37] that a buoyancy parameter $\xi(x)=\frac{Gr_x}{\mathrm{Re}_x^2}$ which in this problem it is also the nonsimilarity variable. ξ>0 is for buoyancy that assisting the flow and ξ<0 for buoyancy opposing the force flow. The parameters are defined as

$M=\frac{\sigma B_0^2 x}{U\rho_{nf}}$ (Magnetic parameter)

$Gr_x=\frac{g\beta(T_w-T_\infty)x^3}{v_f^2}$ (Grashof number)

$\mathrm{Re}_x=\frac{U_\infty x}{v_f}$ (Reynolds number)

$\mathrm{Pr}=\frac{v_f}{\alpha}$ (Prandtl number)

$N=\frac{16\sigma_1 T_\infty^3}{3k_1k_{nf}}$ (Thermal radiation parameter)

Noted that when ξ=0, there is no buoyancy force and the system reduce to pure force convection problem. The transformed boundary conditions are

$$\eta=0: f'(\xi,0)=0, f(\xi,0)=2s-2\xi\frac{\partial f}{\partial\xi},\theta(\xi,0)=1$$

$$\eta\to\infty: f'(\xi,\infty)=1,\ \theta(\xi,\infty)=0 \quad (17)$$

where prime denote differentiation with respect to η and s (suction parameter) is defined as

$$s = \frac{v_0 x}{(v_f U x)^{1/2}}$$

such that (S>0) and (S=0) for an impermeable surface. We may observe that after transformation, Equs. (15)-(17) still containing ∂/∂ξ. It is obvious that this problem is a nonsimilarity boundary layer problem and need to be solved using local nonsimilarity solution method.

## Local Non-similarity Method

One frequently-used concept in the solution of nonsimilarity boundary layers is the principle of local similarity. According to this concept, the right-hand sides of equations (15) and (16) are assumed to be sufficiently small so that it may be approximated by zero, resulting a system of ordinary differential equations and the computational task is simplified [28]. Therefore, the local similarity solution or the first level of truncation is computationally attractive but leads to numerical results of uncertain accuracy. This is due to the uncertainty on whether to neglect the right-hand side of the equations or not when ξ is not small [38]. In order to overcome such a drawback, Sparrow and Quack [28] and Sparrow and Yu [39] presented the local non-similarity method in obtaining the solutions for the non-similar boundary layer equations. In obtaining the local non-similarity solution of equations (15-17), first, let eliminate the presence of term ∂/∂ξ by defining the new dependent variables as

$$g = \frac{\partial f}{\partial \xi}, \varphi = \frac{\partial \theta}{\partial \xi}, z = \frac{\partial g}{\partial \xi} \text{ and } x = \frac{\partial \varphi}{\partial \xi} \tag{18}$$

After substitution variables (18), Equations (15) and (16) become

$$\frac{1}{(1-\phi)^{2.5}\left[1-\phi+\phi\left(\frac{\rho_s}{\rho_f}\right)\right]} f''' + \frac{1}{2} f f'' + \xi\theta - M(f'-1) = \xi\left[f'g' - gf''\right] \tag{19}$$

$$\frac{1}{pr}\frac{\left(\frac{k_{nf}}{k_f}\right)}{\left[1-\phi+\phi\frac{(\rho C_p)_s}{(\rho C_p)_f}\right]}\theta'' + \frac{1}{2(N+1)}\theta' f = \frac{1}{(N+1)}\xi\left[f'\varphi - \theta' g\right] \tag{20}$$

and its boundary conditions

$$f'(\xi,0) = 0, f(\xi,0) = 2s - 2\xi.g(\xi,0), \theta(\xi,0) = 1,$$

$$f'(\xi,\infty) = 1, \theta(\xi,\infty) = 0 \tag{21}$$

Since g and φ represent two additional unknown functions, it is necessary to deduce two more equations for determining the g and φ. Subsidiary equations for g and φ and their boundary conditions are derived by taking the derivatives of equations (19 & 20) and its boundary conditions, Equ.. (17) with respect to ξ. This leads to

$$\frac{1}{(1-\phi)^{2.5}\left[1-\phi+\phi\left(\frac{\rho_s}{\rho_f}\right)\right]} g''' + \frac{3}{2} f' g + \frac{1}{2} f g'' + \theta + \xi\varphi - Mg' - f'g' = \xi\left[g'g' + f'z' - gg'' - f''z\right] \tag{22}$$

$$\frac{1}{pr}\frac{\left(\frac{k_{nf}}{k_f}\right)}{\left[1-\phi+\phi\frac{(\rho C_p)_s}{(\rho C_p)_f}\right]}\varphi'' + \frac{1}{(N+1)}\left[\frac{1}{2} f\varphi' - f'\varphi + \frac{3}{2}\theta' g\right] = \frac{1}{(N+1)}\xi\left[\varphi g' + f'x - g\varphi' - \theta' z\right] \tag{23}$$

$$g'(\xi,0) = 0; 3g(\xi,0) + 2\xi.z(\xi,0) = 0; \varphi(\xi,0) = 0; g'(\xi,\infty) = 0; \varphi(\xi,\infty) = 0 \tag{24}$$

Equations (22-24) serve as auxiliaries to the governing equations (Equs. (19-21). It should be pointed out that this form of local non-similarity solutions is also known as the second level of truncation or also referred as two-equation local nonsimilarity model [28]. To carry this method to the third level of truncation (or three-equation model), in a similar manner, we differentiated the auxiliary equations (Equs. (22-24) with respect to ξ, while the governing equations and their boundary conditions are retained without approximation [39]. This yield the following equations and boundary conditions

$$\frac{1}{(1-\phi)^{2.5}\left[1-\phi+\phi\left(\frac{\rho_s}{\rho_f}\right)\right]} z''' + 3gg'' + \frac{5}{2} f''z + \frac{1}{2} fz'' + 2\varphi + \xi x - Mz' \tag{25}$$

$$-2g'g' - 2f'z' = \xi\left[3g'z' - g'z' - 2zg'' + f'\frac{\partial z''}{\partial \xi} - f''\frac{\partial z}{\partial \xi}\right]$$

$$\frac{1}{pr}\frac{\left(\frac{k_{nf}}{k_f}\right)}{\left[1-\phi+\phi\frac{(\rho C_p)_s}{(\rho C_p)_f}\right]}\chi'' + \frac{1}{(N+1)}\left[3\varphi' g + \frac{1}{2} f\chi' - 2\varphi g' - 2f''\chi + \frac{5}{2}\theta'' z\right] \tag{26}$$

$$= \frac{1}{(N+1)}\xi\left[2g'\chi + \varphi z' - 2z\varphi' - g\chi'' + f''\frac{\partial \chi}{\partial \xi} - \theta'\frac{\partial z}{\partial \xi}\right]$$

$$z'(\xi,0) = 0; 5z(\xi,0) + 2\xi.\frac{\partial z}{\partial \xi}(\xi,0) = 0; \chi(\xi,0) = 0; z'(\xi,\infty) = 0; \chi(\xi,\infty) = 0 \tag{27}$$

In order to complete the formulation of the three-equation model, following Chen [40], terms involving $\xi\frac{\partial z}{\partial \xi}, \xi\frac{\partial z}{\partial \xi}$ and $\xi\frac{\partial \chi}{\partial \xi}$ are deleted from equations (25-27). The rationale for this reduction is similar to the concept in deriving the local similarity model but with a fundamental difference in the outcome. In local similarity model, it was postulated that derivatives involving ∂/∂ξ are very small when ξ is not small. Similarly, in reducing Equs. (25-27), it was postulated that the derivatives of the auxiliary functions $\left[\frac{\partial}{\partial \xi}(z), \frac{\partial}{\partial \xi}(z') \text{ and } \frac{\partial}{\partial \xi}(\chi)\right]$ are sufficiently small for ξ values not near zero so that they may be neglected [39]. In the case of local similarity model, the outcome is that a part of the momentum and energy equations itself is lost, but for the local non-similarity approach, the reduction is introduced in a auxiliary equations (Eqns. (25-27), so that the nonsimilarity terms in the governing equations are retained. As a result the local nonsimilarity approach would yield more accurate results compared to the local similarity model [41]. Therefore, the governing equations and its auxiliary equation could be brought together as

$$\frac{1}{(1-\phi)^{2.5}\left[1-\phi+\phi\left(\frac{\rho_s}{\rho_f}\right)\right]} f''' + \frac{1}{2} f f'' + \xi\theta - M(f'-1) = \xi\left[f'g' - gf''\right] \tag{28}$$

$$\frac{1}{pr}\frac{\left(\frac{k_{nf}}{k_f}\right)}{\left[1-\phi+\phi\frac{(\rho C_p)_s}{(\rho C_p)_f}\right]}\theta'' + \frac{1}{2(N+1)}\theta' f = \frac{1}{(N+1)}\xi\left[f''\varphi - \theta'' g\right] \tag{29}$$

$$\frac{1}{(1-\phi)^{2.5}\left[1-\phi+\phi\left(\frac{\rho_s}{\rho_f}\right)\right]} g''' + \frac{3}{2} f''g + \frac{1}{2} fg'' + \theta + \xi\varphi - Mg' - f'g' = \xi\left[g'g' + f'z' - gg'' - f''z\right] \tag{30}$$

$$\frac{1}{pr}\frac{\left(\frac{k_{nf}}{k_f}\right)}{\left[1-\phi+\phi\frac{(\rho C_p)_s}{(\rho C_p)_f}\right]}\varphi''+\frac{1}{(N+1)}\left[\frac{1}{2}f\varphi'-f'\varphi+\frac{3}{2}\theta'g\right]=\frac{1}{(N+1)}\xi\left[\varphi g'+f'\chi-g\varphi'-\theta' z\right] \quad (31)$$

$$\frac{1}{(1-\phi)^{2.5}\left[1-\phi+\phi\left(\frac{\rho_s}{\rho_f}\right)\right]}z''+3gg''+\frac{5}{2}f''z+\frac{1}{2}fz''+2\varphi+\xi\chi-Mz'-2g'g' \quad (32)$$

$$-2f'z'-=\xi\left[3g'z'-gz''-2zg''\right]$$

$$\frac{1}{pr}\frac{\left(\frac{k_{nf}}{k_f}\right)}{\left[1-\phi+\phi\frac{(\rho C_p)_s}{(\rho C_p)_f}\right]}\chi''+\frac{1}{(N+1)}\left[3\varphi'g-\frac{1}{2}f\chi'-2\varphi g'-2f''\chi+\frac{5}{2}\theta''z\right] \quad (33)$$

$$=\frac{1}{(N+1)}\xi\left[2g'\chi+\varphi z'-2z\varphi'-g\chi''\right]$$

subject to the boundary conditions

$$f'(\xi,0)=0;\ f(\xi,0)=2s-2\xi.g(\xi,0),\ \varphi(\xi,0)=1;\ f'(\xi,\infty)=1;\ \varphi(\xi,\infty)=0$$
$$g'(\xi,0)=0;\ 3g(\xi,0)+2\xi.z(\xi,0)=0;\ \varphi(\xi,0)=0;\ g'(\xi,\infty)=0;\ \varphi(\xi,\infty)=0 \quad (34)$$
$$z'(\xi,0)=0;\ 5z(\xi,0)=0;\ \chi(\xi,0)=0;\ z'(\xi,0)=0;\ \chi(\xi,\infty)=0$$

Since the values of the problem parameters are given, these resulting system of equations resembles as a system of ordinary differential equations for function f and θ that contain a parameter ξ which also being treated as buoyancy force. Whether the solution is to be carried out at the first, second or third level of truncation, functions of interest are f(ξ,η), θ(ξ,η) and their derivatives. The major physical quantities of interest are the local skin friction coefficient and the local Nusselt number which are respectively defined by [42]

$$C_f=\frac{\tau_w}{\rho_f U_\infty^2},\ Nu=\frac{h_{tc}x}{k_f} \quad (35)$$

with $\tau_w$, $h_{tc}$ and $k_f$ are the surface shear stress, heat transfer coefficient and thermal conductivity of fluid respectively. Also given that

$$\tau_w=\mu_{nf}\left(\frac{\partial u}{\partial y}\right)_{y=0}\ and\ h_{tc}=\frac{q_w}{(T_w-T_\infty)} \quad (36)$$

where the wall (or surface) heat flux is defined as $q_w=-k_{nf}\left(\frac{\partial T}{\partial y}\right)_{y=0}$.

Both quantities, the local skin friction coefficient and the local Nusselt number can be written in term of velocity gradient and temperature gradient respectively as

$$C_f=\frac{1}{(1-\phi)^{2.5}}\frac{f''(\xi,0)}{\mathrm{Re}_x^{1/2}},\ Nu=-\frac{k_{nf}}{k_f}\frac{\theta''(\xi,0)}{\mathrm{Re}_x^{1/2}} \quad (37)$$

## Results and Discussion

In the present investigation, the results are obtained by two different methodologies namely the Runge-Kutta-Gill integration scheme in conjunction with the shooting method and the three-equation local nonsimilarity model method. The two-point boundary value problem of the non similar system of ordinary differential equations has been obtained by the Falkner-Skan transformation. The results are presented graphically for dimensionless velocity and temperature distribution for various prescribed parameters, namely the magnetic parameter M, thermal radiation parameter N, nanoparticles volume fraction ϕ, suction parametes s and the buoyancy parameter ξ. The validation of the present results has been verified with the case of a regular Newtonian fluid (ϕ=0) and no suction/injection, no magnetic effect and no thermal radiation, which first studied by Minkowycz and Sparrow [43]. We have compared steady-state results on skin friction, f''(0) and the rate of heat transfer, -θ'(0) for various value of ξ. The results are found in excellent agreement and the comparisons are shown in Table 1.

Five different types of nanoparticles were considered as listed in Table 2, with water as the base fluid. Thermophysical properties of the nanoparticles and base fluid are listed in Table 2 [14]. Following Oztop and Abu-Nada [7], the Prandtl number Pr of base fluid is kept constant as 6.2. The effects of some prescribed parameters are presented graphically in Figures 2-12.

The effects of buoyancy parameter on dimensionless velocity over a vertical plate in the presence of magnetic and radiation for Cu-water nanofluid are shown in Figure 2 and 3. It is an interesting note from Figure 2 and 3 that the increasing of assisting buoyancy flow (ξ>0), the fluid velocity inside the boundary layer increases and whereas increasing in the opposing flow (ξ<0) decreases the magnitude of the velocity profiles. From the definition of buoyancy parameter

| $\xi=Gr_x/Re^2_x$ | Minkowycz and Sparrow [43] | | Present work | |
|---|---|---|---|---|
| | f''(ξ,0) | –θ'(ξ,0) | f''(ξ,0) | –θ'(ξ,0) |
| 0 | 0.33206 | 0.29268 | 0.3320573 | 0.2926804 |
| 0.4 | 0.73916 | 0.35774 | 0.7391622 | 0.3577421 |
| 1.0 | 1.21795 | 0.41054 | 1.2179529 | 0.4105355 |
| 1.5 | 1.56566 | 0.44106 | 1.5656630 | 0.4410137 |
| 2.5 | 2.18819 | 0.48619 | 2.1881869 | 0.4861908 |
| 5.0 | 3.52696 | 0.56067 | 3.5269162 | 0.5606733 |
| 7.0 | 4.47647 | 0.60283 | 4.4764563 | 0.6028282 |

**Table 1:** Comparison of the values of f''(ξ,0) and –θ'(ξ,0) for various values of ξ.

| Physical properties | $C_p$ (J/kg K) | ρ (kg/m³) | k (W/ mK) | α=k/((ρCp) |
|---|---|---|---|---|
| Water | 4179 | 997.1 | 0.613 | -1.163 |
| Cu (Copper) | 385 | 8933 | 400 | $1.163X10^{-4}$ |
| $Al_2O_3$ (Alumina) | 765 | 3970 | 40 | $1.317X10^{-5}$ |
| $TiO_2$ (Titanium) | 686.2 | 4250 | 8.9538 | $3.070X10^{-6}$ |
| CuO (Copper oxide) | 540 | 6510 | 18 | $5.120X10^{-6}$ |
| Ag (Silver) | 235 | 10500 | 429 | $1.739X10^{-4}$ |

**Table 2:** Thermophysical properties of fluid and nanoparticles [8].

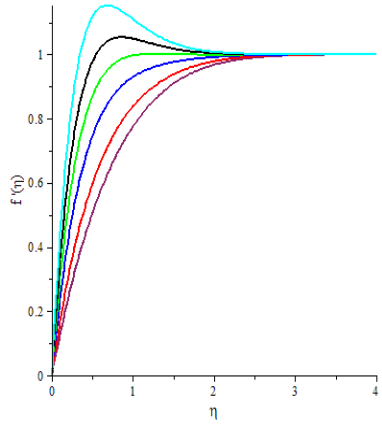


**Figure 2:** Velocity profiles for various positive values of the buoyancy parameter ξ ϕ=0.1, M=0.5, N=0.5 and S=0.5.

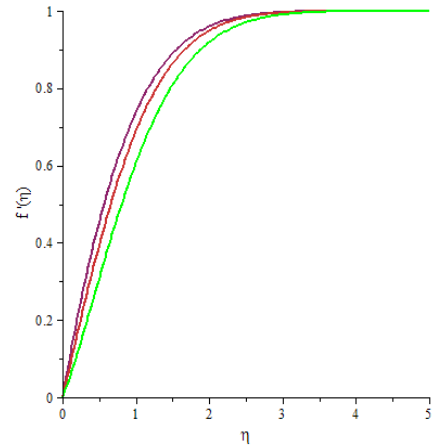


**Figure 3:** Velocity profiles for various negative values of the buoyancy parameter ξ ϕ=0.1, M=0.5, N=0.5 and S=0.5.

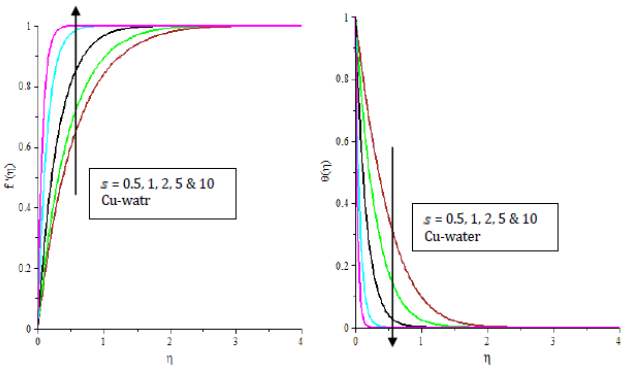


**Figure 4:** Effect of suction, Son velocity and temperature profile ξ=1, M=0.5, N=0.5 and φ=0.1.

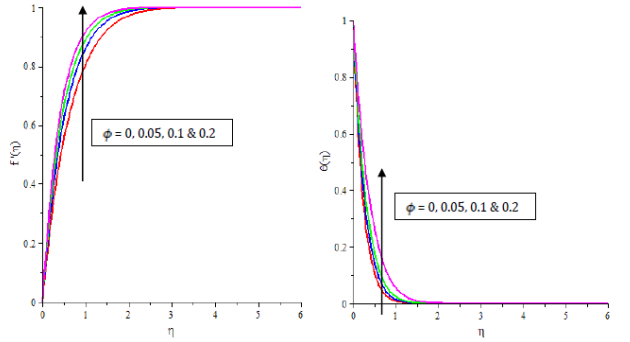


**Figure 5:** Velocity and temperature profiles for various values of ϕξ=0.1, M=0.5, N=0.5 and S=1.

$\left[\xi = \frac{Gr_x}{\mathrm{Re}_x^2} = ax\right]$ (a constant), variation of ξ actually means variation of the distance along the surface. This shows that an assisting buoyancy force acts like a favorable pressure gradient meanwhile the opposing buoyancy force retard the velocity of the flow. The effect of buoyancy forces plays an important role on the displacement of one liquid by another in a consolidated porous medium. The effect of ξ is insignificant in temperature profiles because ξ does not appear directly in the energy Equ. (9). Moreover, the effect of higher Prandtl number results into thinner thermal boundary layer as the higher Prandtl number has a lower thermal conductivity.

Figure 4 depict the influence of the suction parameter (S>0) on velocity and temperature profiles in the presence of buoyancy force and thermal radiation of Cu-water nanofluid. With the increasing in the values of suction, the velocity is found to increase, i.e., suction causes to increase the velocity of the fluid in the boundary layer region. While, for the temperature profiles it is observed that increasing S will decreases the temperature distribution inside the boundary layer. In the presence

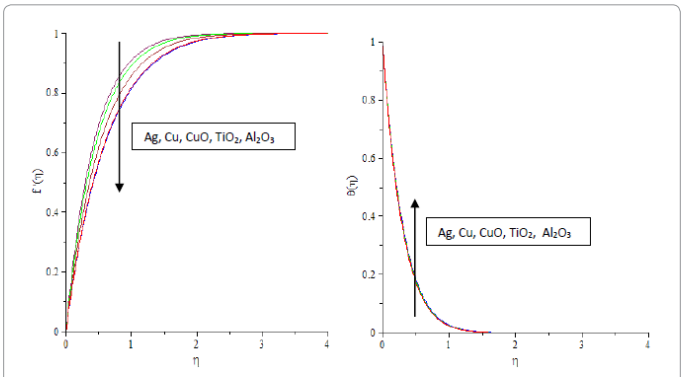


**Figure 6:** Velocity and temperature profiles for different nanoparticles ξ=0.1, M=0.5, N=0.5,φ=0.1 and S=1.

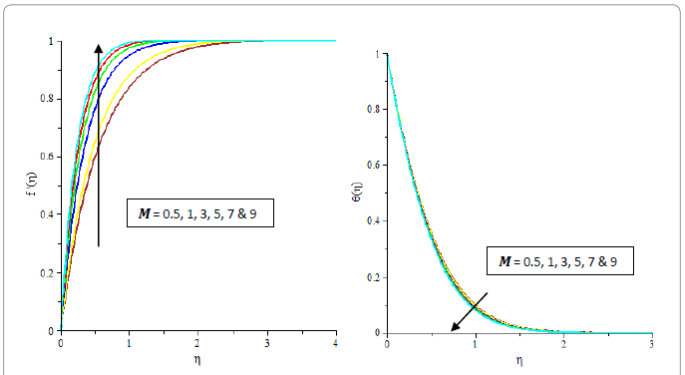


**Figure 7:** Magnetic effect on velocity and temperature profiles ξ=1, N=0.5,φ=0.1 and S=0.5.

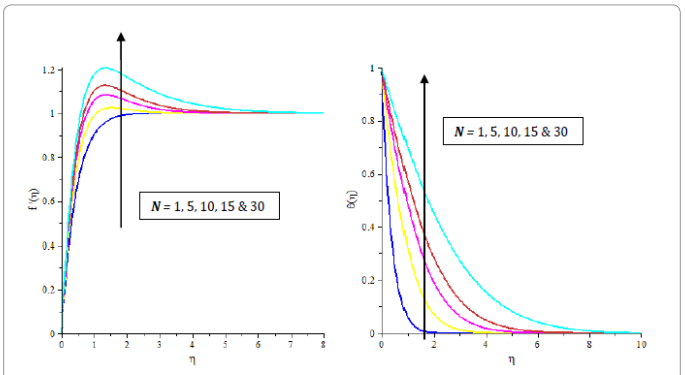


**Figure 8:** Effect of thermal radiation on velocity and temperature profiles when ξ=1,M=0.5, φ=0.1 and S=0.5.

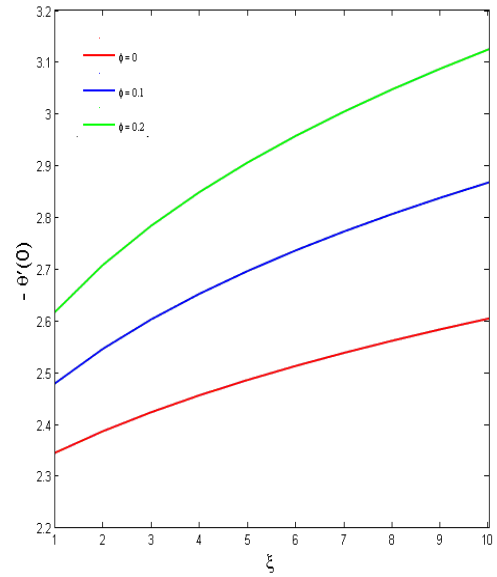


**Figure 9:** Variation of -θ'(0) with positive values of ξ for different values of ϕ when Pr = 6.2and S = 0.2 for Cu-water.

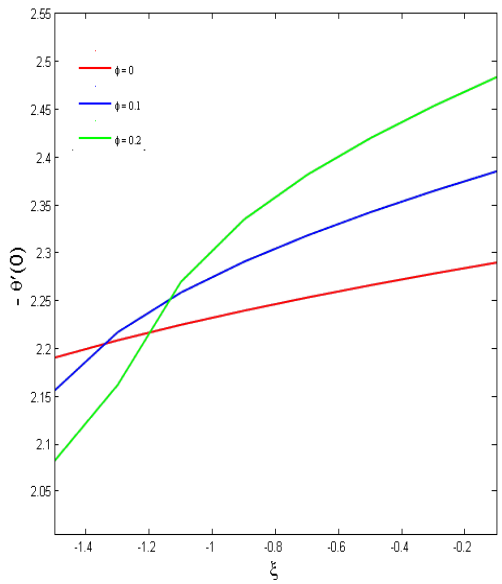


**Figure 10:** Variation of -θ'(0) with negative valuesof ξ for different values of ϕ when Pr = 6.2and S = 0.2 for Cu-water.

of suction, the heated fluid is pushed towards the wall thus reduces the thermal boundary layer thickness i.e., thins out the thermal boundary layers. Thus the presence of suction decreases the momentum boundary layer thickness but increases the thermal boundary layer thickness. The application of suction through the walls is a well known and effective method for postponing transition (Figures 2-5).

Figure 5 is presented to show the effect of nanoparticle volume fraction parameter ϕ on velocity and temperature profiles in the presence of Cu-water nanofluid. In these figures, it is seen that when volume fraction of the nanoparticles increase from 0 to 0.2, the velocity increases inside the boundary layer which may due to the increasing of the viscosity of the fluid. Referring to Equ. (2), its clearly shown that the velocity is linearly proportional to the fluid viscosity. This means that when the fluid viscosity increases, it will increase the fluid velocity. Also it is observed that with increasing the volume fraction of nanoparticles, the temperature distribution inside boundary layer is increased. This agrees with the physical behavior that when the volume fraction of nanoparticles increases, the density and thermal conductivity of the nanofluid would increases. The stochastic motion of nanoparticles could be an explanation to the thermal conductivity enhancement since smaller particles are more easily to mobilize and causes a higher level of stochastic motion.

Figure 6 represents the velocity and temperature profiles using different types of nanoparticles (Ag, Cu, CuO, $Al_2O_3$ and $TiO_2$) when ξ=1, φ=0.1 and s=0.1. It was noticed that the velocity distribution

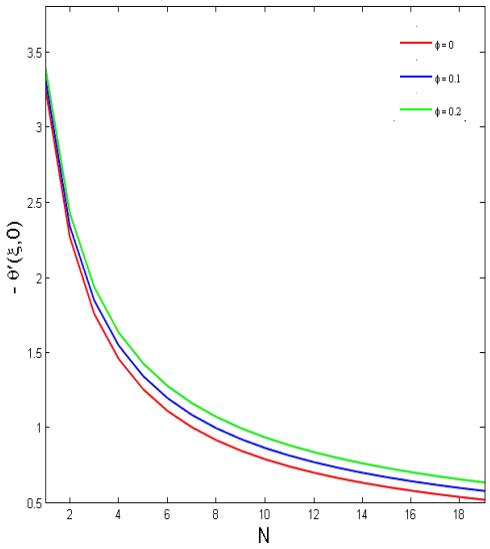


**Figure 11:** Variation of -θ'(0) with N for different values of ϕ when Pr = 6.2 and S = 0.2 for Cu-water.

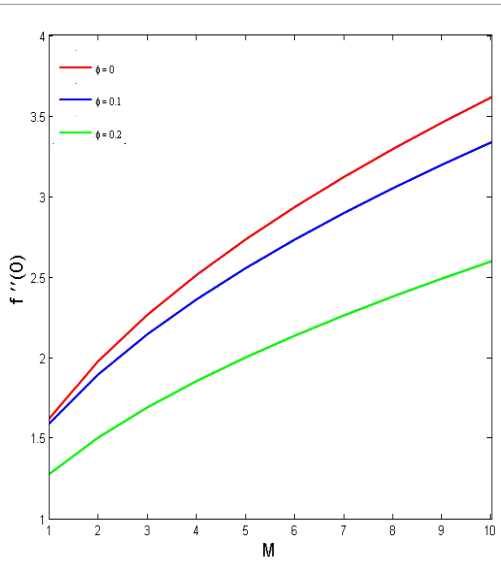


**Figure 12:** Variation of -θ'(0) with Mfor different values of ϕ when Pr = 6.2 and S = 0.2 for Cu-water.

of Silver nanofluid (Ag-water) is higher compared to all the other nanofluids. This behavior due to the combined effect of density and thermal diffusivity of Ag-nanofluid as can be seen in Table 2. Higher thermal diffusivity means a higher conductivity compared to heat capacity. This means that the material transfer more heat to the surrounding touching the material rather than stores it. Therefore, the heat that was absorbed by the particles would increase the level of kinetic energy of the particles and indirectly would decreases the viscosity of the nanofluid and therefore increase the velocity of the flow. On the other hand, since silver has the highest thermal conductivity, then this particles has the lowest temperature distribution inside the boundary layer compared to other nanofluids, Higher thermal conductivity means higher heat transfer rate.

Figure 7 presents typical profiles for velocity and temperature for different values of magnetic parameter. It is observed that an increase in the value of magnetic field, M increases the fluid velocity inside the boundary layer but has no significant effect on the fluid temperature distribution. Meanwhile, the effects of thermal radiation, N, on velocity and temperature profiles of Cu-water nanofluid are illustrated in Figure 8 in the case of uniform suction and magnetic field. It is observed that both the velocity and temperature of the nanofluid increases with the increase of radiation parameter N. This result can be explained by the definition in the value of $N = \frac{4\sigma_1\theta^3}{k^*(\sigma C_p)_f}$. Since N is linearly proportional with temperature, increasing in N will increase the temperature distribution in the boundary layer region.

In the presence of aiding buoyancy force $\xi>0$, it is predicted that the rate of heat transfer of Cu-nanofluid increases with increase of nanoparticle volume fraction whereas the rate of heat transfer firstly decreases and then increases with increase of nanoparticle volume fraction in the presence of aiding buoyancy force $\xi<0$. All these physical behaviour are the combined effects of the strength of density, kinematic viscosity and thermal conductivity of Cu-nanofluid (Figures 9 and 10).

In the presence of thermal radiation, it is observed that the rate of heat transfer of Cu-nanofluid increases with increase of nanoparticle volume fraction because of the combined effects of thermal conductivity and the kinematic viscosity of the cu-nanofluid whereas the rate of heat transfer decreases with increase of nanoparticle volume fraction in the presence of magnetic parameter. All these are the joined effects of density and electrical conductivity of the Cu-nanofluid (Figures 11 and 12).

## Conclusion

In the present paper, we have examined the influence of the different type of nanoparticles on boundary layer flow and heat transfer of incompressible nanofluid along the permeable vertical plate with thermal radiation in the presence of magnetic field. The governing partial differential equations for mass, momentum and energy conservation are transformed into ordinary differential equations by using a non-dimensional local non similarity transformation. These equations are solved numerically using Runge-Kutta-Gill integration scheme in conjunction with the shooting method. The two-point boundary value problem of the non similar system of ordinary differential equations has been obtained by the Falkner-Skan transformation. The effects of the magnetic parameter M, thermal radiation parameter N, suction parameter S, the buoyancy parameter $\xi$ and nanoparticles volume fraction $\phi$ of Cu-nanofluid and different types of nanofluids (Ag, CuO, $Al_2O_3$, $TiO_2$) are discussed. Numerical results for the skin friction, rate of heat transfer, temperature and velocity are presented graphically for various parameter conditions.

The results can be summarized as follows:

1. Physically, it is interesting to note that the increase of momentum/thermal boundary layer field due to increase in nanoparticle volume fraction parameter shows that the velocity/temperature decreases/increases gradually as we replace Ag, Cu, CuO, $TiO_2$ and $Al_2O_3$ in the said sequence. It implies that the thermal conductivity of nanofluid is strongly dependent on the nanoparticle volume fraction.

2. It is predicted that the velocity/temperature of Cu-nanofluid increases/decreases with increase of magnetic strength because of the transport properties of the copper nanofluid. Copper nanoparticles in the magnetic field are a unique material that has both the nanofluid and magnetic properties.

3. It is noticed that the velocity and temperature of the copper nanofluid is accelerated significantly with increase of convective radiation because of decrease of thermal conductivity of the copper nanoparticles is to decrease the rate of energy transport to the copper nanofluid.

4. In the presence of thermal radiation/magnetic field, the rate of heat transfer of Cu-nanofluid increases/decreases with increase of nanoparticle volume fraction. All these are the joined effects of kinematic viscosity and thermal and electrical conductivity of the Cu-nanofluid.

5. In the presence of aiding buoyancy force, the rate of heat transfer of Cu-nanofluid increases with increase of nanoparticle volume fraction because of the combined effects of the strength of density and thermal conductivity of the Cu-nanofluid.

6. It is observed that the velocity/temperature of the Cu-nanofluid increases/decreases with increase of suction parameter. This is due to the fact that the heated fluid is pushed towards the wall thus reduces the thermal boundary layer thickness i.e., thins out the thermal boundary layers.

7. It is observed that the velocity of the Cu-nanofluid increases/decreases with increase of assisting buoyancy flow ($\xi>0$) opposing buoyancy flow ($\xi<0$) respectively. This shows that an assisting buoyancy force acts like a favorable pressure gradient meanwhile the opposing buoyancy force retard the velocity of the flow. The effect of $\xi$ is insignificant in temperature profiles because $\xi$ does not appear directly in the energy Equ. (9).

8. It is interesting to note that the velocity and the temperature of the Cu-nanofluid increase with increase of nanoparticle volume fraction which may due to the combined effect of density and thermal conductivity of the Cu-nanofluid. The stochastic motion of nanoparticles could be an explanation to the thermal conductivity enhancement since smaller particles are more easily to mobilize and causes a higher level of stochastic motion.

It is concluded that the novel and advanced concepts of nanofluids offer fascinating heat transfer characteristics compared to conventional heat transfer fluids. There are considerable researches on the superior heat transfer properties of nanofluids especially on thermal conductivity and convective heat transfer. Applications of nanofluids in industries such as heat exchanging devices appear promising with these characteristics. The increases in effective thermal conductivity are important in improving the heat transfer behavior of fluids. An in-depth understanding of the interactions between particles, stabilizers, the suspending liquid and the heating surface will be important for applications.

## References

1. Ebrahimi S, Gavili A, Lajevardi M, Isfahani TD, Hadi I, et al. (2010) New Class of Coolants-Nanofluids in Cutting Edge Nanotechnology, Vasileska D (eds.). InTech.
2. Trisaksri V, Wongwises S (2007) Critical review of heat transfer characteristics of nanofluids. Renewable and Sustainable Energy Reviews 11: 512-523.
3. Sreenavasulu P, Reddy NB (2013) Thermal Radiation and Chemical Reaction Effects on Mhd Stagnation-Point Flow of a Nanofluid over a Porous Stretching Sheet Embedded in a Porous Medium with Heat Absorption/Generation-Lie Group Analysis. Journal of Global Research in Mathematical Archives 1: 13-27.
4. Abu-Nada E (2008) Application of nanofluids for heat transfer enhancement of separated flow encountered in a backward facing step. Int. J. Heat Fluid Flow 29: 242-249.
5. Maiga SEB, Palma SJ, Nguyena CT, Roya G, Galanisb N (2005) Heat transfer enhancement by using nanofluids in forced convection flows. Int. Journal Heat Fluid Flow 26: 530-546.
6. Polidari G, Fohanno S, Nguyen CT (2007) A note on heat transfer modeling of Newtonian nanofluids in laminar free convection. Int. Journal Thermal Sciences 46: 739-744.
7. Oztop HF, Abu-Nada E (2008) Numerical study of natural convection in partially heated rectangular enclosures filled with nanofluids. Int. Journal Heat Fluid Flow 29: 1326-1336.
8. Nield DA, Kuznetsov AV (2009) The Cheng-Minkowycz problem for natural convective boundary-layer flow in a porous medium saturated by a nanofluid. Int. Journal of Heat and Mass Transfer 52: 5792-5795.
9. Kuznetsov AV, Nield DA (2010) Natural convective boundary-layer flow of a nanofluid past a vertical plate. Int J Thermal Sci 49: 243-247.
10. Muthtamilselvan M, Kandaswamy P, Lee J (2010) Heat Transfer Enhancement of Copper-Water Nanofluids-In A Lid-Driven Enclosure. Commun. Nonlinear Sci Numer Simulat 15: 1501-1510.
11. Yacob NA, Ishak A, Pop I (2011) Falkner-Skan problem for a static or moving wedge in nanofluids. Int. Journal of Thermal Sciences 50: 133-139.
12. Jacob K, Wabomba MS, Kinyanjui AM, Lunani MA (2012) Magnetic Field and Hall Current Effect on MHD Free Convection Flow Past A Vertical Rotating Flat Plate. Asian Journal of Current Engineering and Maths 1: 346 - 354.
13. Nadeem S, Ul Haq R (2014) Effect of Thermal Radiation for Magnetohydrodynamic Boundary Layer Flow of a Nanofluid Past a Stretching Sheet with Convective Boundary Conditions. Journal of Computational and Theoretical Nanoscience 11: 32-40.
14. Hamad MAA, Pop I, Ismail MAI (2010) Magnetic field effects on free convection flow of a nanofluid past a vertical semi-infinite flat plate. Nonlinear Analysis: Real World Applications 12: 1338-1346.
15. Chamka AJ, Aly AM (2010) MHD Free Convection Flow of a Nanofluid Past a Vertical Plate in the Presence of Heat Generation or Absorption Effects. Chemical Engineering Communications 198: 425-441.
16. Uddin MJ, Khan WA, Ismail AI (2012) MHD Free Convective Boundary Layer Flow of a Nanofluid past a Flat Vertical Plate with Newtonian Heating Boundary Condition. Plos One 7: 1-8.
17. Ibrahim W, Shanker B (2014) Magnetohydrodynamic Boundary Layer Flow and Heat Transfer of a Nanofluid Over Non-Isothermal Stretching Sheet. Journal of Heat Transfer 136(5): 1-9.
18. Makinde OD, Aziz A (2011) Boundary layer flow of a nanofluid past a stretching sheet with a convective boundary condition. International Journal of Thermal Sciences 50(7): 1326–1332.
19. AbdEl-Gaied SM, Hamad MAA (2013) MHD Forced Convection Laminar Boundary Layer Flow of Alumina-Water Nanofluid over a Moving Permeable Flat Plate with Convective Surface Boundary Condition. Journal of Applied Mathematics 2013: 1-9.
20. Matin MH, Jahangiri P (2014) Forced Convection Boundary Layer Magnetohydrodynamic Flow of Nanofluid over a Permeable Stretching Plate with Viscous Dissipation. Thermal Science 18: S587-S598.
21. Keshtkar MM, Esmaili N, Ghazanfari MR (2014) Effect of heat source/sink on mhd mixed convection boundary layer flow on a vertical surface in a porous medium saturated by a nanofluid with suction or injection. International Journal of Engineering and Science 4: 1-11.
22. Khan MS, Karim I, Islam MS, Wahiduzzaman M (2014) MHD Boundary Layer Radiative, Heat Generating and Chemical Reacting Flow Past a Wedge Moving in a Nanofluid. Nano Convergence 1: 1-13.
23. Poornima T, Reddy NB (2013) Radiation effects on MHD free convective boundary layer flow of nanofluids over a nonlinear stretching sheet. Advances in Applied Science Research 4: 190-202.
24. Aini Mat NA, Arifin NM, Nazar R, Ismail F, Bachok N (2013) MHD mixed convection flow of a power law nanofluid over a vertical stretching sheet with radiation effect. AIP Conference Proceedings 1557: 604.
25. Shateyi S, Prakash J (2014) A New numerical approach for mhd laminar boundary layer flow and heat transfer of nanofluids over a moving surface in the presence of thermal radiation. Boundary Value Problems 2: 1-12.
26. Reddy MG (2014) Influence of Magnetohydrodynamic and Thermal Radiation Boundary Layer Flow of a Nanofluid Past A Stretching Sheet. Journal of Scientific Research 6: 257-272.
27. Haile E, Shankar B (2014) A Steady Mhd Boundary-Layer Flow of Water-Based Nanofluids Over a Moving Permeable Flat Plate. International Journal of Mathematical Research 4: 27- 41.
28. Sparrow EM, Quack H, Boerner CJ (1970) Local Nonsimilarity Boundary-Layer Solutions. AIAA Journal 8: 1936-1942.
29. Muhaimin I, Kandasamy R (2010) Local Nonsimilarity Solution for the Impact of a Chemical Reaction in an MHD Mixed Convection Heat and Mass Transfer Flow over a Porous Wedge in the Presence of Suction/injection. Journal of Applied Mechanics and Technical Physics 51: 721-731.
30. Akgul MB, Pakdemirli M (2012) Cooling Intensification of a Continuously Moving Stretching Surface Using Different types of Nanofluids. Journal of Applied Mathematics pp: 11.
31. Watanabe T (1991) Forced and Free Mixed Convection Boundary Layer Flow with Uniform Suction or Injection on A Vertical Flat Plate. Aeta Mechanica 89: 123-132.
32. Tiwari RJ, Das MK (2007) Heat Transfer augmentation in a two-sided lid-driven differentially heated square cavity utilizing nanofluids. Int. Journal Heat Mass Transfer 50: 2002-2018.
33. Brinkman HC (1952) The Viscosity of Concentrated Suspensions and Solutions. J Chem Phys 20: 571-581.
34. Bachok N, Ishak A, Pop I (2012) Boundary layer flow over a moving surface in a nanofluid with suction or injection. Acta Mech Sin 28: 34-40.
35. Aminossadati SM, Ghasemi B (2009) Natural convection cooling of a localized heat source at the bottom of a nanofluid-filled enclosure. Eur J Mech B Fluids 28: 630-640.
36. Maleque KA (2013) Effects of Exothermic/Endothermic Chemical Reactions with Arrhenius Activation Energy on MHD Free Convection and Mass Transfer Flow in Presence of Thermal Radiation. Journal of Thermodynamics pp: 1-11.
37. Siddiqa S, Hossain MA (2012) Mixed Convection Boundary Layer Flow over a Vertical Flat Plate with Radiative Heat Transfer. Applied Mathematics 3: 705-716.
38. Yian LY, Amin N (2002) Local Nonsimilarity Solution for Vertical Free Convection Boundary Layers. Matematika 18: 21-31.
39. Sparrow EM, Yu HS (1971) Local Non-Similarity Thermal Boundary-Layer Solutions. ASME Journal 328-334.
40. Chen TS (1988) Parabolic System-Local Non similarity Method in Handbook of Numerical Heat Transfer. Wiley-Interscience, New York.
41. Massoudi M (2001) Local Non-Similarity Solutions for the Flow of a Non-Newtonian Fluid over a Wedge. International Journal of Non-Linear Mechanics 36: 961-976.
42. Muhaimin I, Kandasamy R, Loganathan P, Arasu PP (2012) Local Non-similarity Solution for the Impact of the Buoyancy Force on Heat and Mass Transfer in a Flow Over a Porous Wedge with a Heat Source in the Presence of Suction/Injection. Journal of Applied Mechanics and Technical Physics 53: 231-241.
43. Minkowycz WJ, Sparrow EM (1978) Numerical Solution Scheme for Local Nonsimilarity Boundary-Layer Analysis. Numerical Heat Transfer 1: 69-85.